# Radiologic Evaluation

2

David A. Lynch

**Abstract**

High resolution CT is useful for early detection and characterization of diffuse lung diseases. Optimal CT evaluation requires careful attention to technique. Radiologic diagnosis is based on the use of standard descriptive terms and the distribution of abnormality in the craniocaudal and axial planes. Confident CT diagnoses of several diffuse diseases, including usual interstitial pneumonia, sarcoidosis, hypersensitivity pneumonitis, smoking-related lung injury, Langerhans histiocytosis, lymphangioleiomyomatosis, based on typical CT findings and made in the appropriate clinical context, are usually correct. However, certain other radiologic findings, particularly ground-glass abnormality, consolidation and reticular abnormality, are relatively nonspecific and will usually require further diagnostic evaluation.

**Keywords**

High resolution CT • Diagnosis • Usual interstitial pneumonia • Sarcoidosis • Hypersensitivity pneumonitis

## Introduction

The purposes of this chapter are to explain optimal CT technique to evaluate diffuse lung disease, to describe and illustrate the common radiologic signs of diffuse lung disease, and to show how imaging can help elucidate some common clinical problems.

D.A. Lynch (✉)
Department of Radiology, National Jewish Health, Denver, CO, USA
e-mail: lynchd@njhealth.org

## CT Techniques

The technique of high resolution CT (HRCT) requires thin (1–1.5 mm) sections and a special reconstruction algorithm to maximize detail in the lung parenchyma [1] (Fig. 2.1). HRCT images may be reconstructed from a volumetric dataset or may be acquired using noncontiguous images at 1–2 cm intervals. If volumetric acquisition is performed, coronal and sagittal reconstructions may be obtained, and may be very helpful in understanding distribution of disease.

Careful attention to technique is required to ensure high quality images. In particular,

R.P. Baughman and R.M. du Bois (eds.), *Diffuse Lung Disease: A Practical Approach*,
DOI 10.1007/978-1-4419-9771-5_2, 

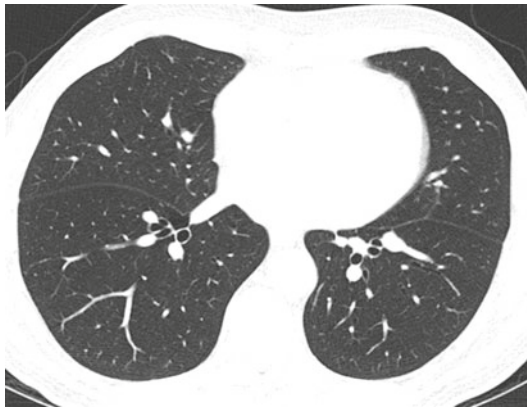

**Fig. 2.1** Normal high resolution CT

technologists must work with the patient to ensure the absence of respiratory motion, which is the commonest cause of suboptimal images. Because atelectasis in the dependent lung can obscure detail, prone HRCT imaging is frequently performed to evaluate the posterior lung, where the early changes of asbestosis, collagen vascular-related lung disease, and idiopathic interstitial pneumonias may be first seen. Expiratory CT is often pivotal in identifying gas trapping in obstructive lung disease and hypersensitivity pneumonitis and sarcoidosis.

## Radiologic Signs of Diffuse Lung Disease

Specificity of radiologic descriptors enhances the ability of radiologists to communicate their findings and generate appropriate differential diagnoses. The Fleischner Society has published a helpful glossary of descriptors used in thoracic imaging, which serves as standardized terminology [2]. Nonspecific terms such as alveolitis are best avoided. Table 2.1 illustrates the differential diagnosis of common patterns in diffuse lung disease.

### Consolidation/Ground-Glass Attenuation

The term parenchymal opacification [3, 4] is applied to any homogeneous increase in lung density on chest radiographs or chest CT. When this parenchymal opacification is dense enough to obscure the vessels and other parenchymal structures, it is called *consolidation* (Fig. 2.2). Since consolidation is usually due to a pathologic process filling the alveoli its differential diagnosis is broad, but may be narrowed when seen in relatively healthy outpatients, as given in Table 2.1.

*Ground-glass attenuation* is defined as an increase in lung density not sufficient to obscure vessels (see Fig. 2.2). Ground-glass attenuation is commonly, though not always, associated with reversible or potentially reversible lung disease. Because ground-glass attenuation may be due to any infiltrative process involving alveoli or alveolar septa, the differential diagnosis is broad. The differential presented in Table 2.1 may be applied to relatively healthy outpatients.

### Nodules

Nodules seen on HRCT can be classified according to their size (micronodules or larger nodules), density (ground glass, soft tissue, or calcific densities), definition (well defined or poorly defined), and distribution. Micronodules measure less than 3 mm in diameter [5]. Gruden et al. [6] classified nodules on the basis of their location (random, perilymphatic, centrilobular, or airways associated). Perilymphatic micronodules are seen in subpleural and septal locations, most commonly in subjects with sarcoidosis (Fig. 2.3) or lymphangitic carcinoma, but may also be seen in pneumoconiosis. Scattered subpleural micronodules may be seen in normal subjects. Centrilobular nodules (see Table 2.2) are recognized by their characteristic location (Fig. 2.4), approximately 1–2 mm from each other, and separated by about the same distance from pleura and vessels. They are often of ground-glass attenuation. Small airways-associated nodules are identified when the tree-in-bud pattern is present (nodules closely related to small branching structures) (Fig. 2.5). These nodules are usually centrilobular.

Nodules of ground-glass density are typically seen in hypersensitivity pneumonitis (see Fig. 2.4), but may also be seen in respiratory bronchiolitis. Soft tissue density nodules are seen in patients with granulomatous lung diseases, malignancy,

**Table 2.1** Differential diagnosis of infiltrative lung disease based on CT pattern

| CT findings | Differential diagnosis |
|---|---|
| Consolidation[a] | Chronic infection (mycobacterial, fungal) |
| | Organizing pneumonia |
| | Sarcoidosis (pseudoalveolar) |
| | Bronchioloalveolar carcinoma |
| | Lymphoma |
| | Eosinophilic pneumonia |
| | Vasculitis |
| | Chronic aspiration (esp. lipid) |
| Ground-glass attenuation[a] | Hypersensitivity pneumonitis |
| | Nonspecific interstitial pneumonia |
| | Desquamative interstitial pneumonitis/respiratory bronchiolitis interstitial lung disease |
| | Hemorrhage |
| | Eosinophilic pneumonia |
| | Drug toxicity |
| Nodules | Malignancy |
| | Silicosis |
| | Coal workers' pneumoconiosis |
| | Granulomatous infection |
| | Sarcoidosis |
| | Berylliosis |
| | Langerhans cell histiocytosis |
| | Centrilobular nodules (see Table 2.3) |
| Fibrotic disease (reticular pattern, traction bronchiectasis, architectural distortion) | Usual interstitial pneumonia |
| | Nonspecific interstitial pneumonia |
| | Asbestosis |
| | Collagen vascular disease |
| | Sarcoidosis |
| | Chronic hypersensitivity pneumonitis |
| Honeycombing | Usual interstitial pneumonia |
| | Sarcoidosis |
| Cysts | Lymphangioleiomyomatosis |
| | Langerhans cell histiocytosis |
| | Lymphoid interstitial pneumonia |
| | Desquamative interstitial pneumonia |
| Crazy paving pattern[a] | Pulmonary alveolar proteinosis |
| | Lipoid pneumonia |
| | Bronchioloalveolar carcinoma |
| Decreased lung attenuation/mosaic attenuation | Hypersensitivity pneumonitis |
| | Obliterative bronchiolitis |
| | Thromboembolic disease |
| | Panlobular emphysema |

Adapted from Lynch DA. Imaging of diffuse parenchymal lung diseases. In: Schwarz M, King T, editors. Interstitial lung disease. 5th ed. McGraw Hill; 2011. p. 105–49.

[a]The differential diagnosis provided here for consolidation, ground-glass attenuation, and crazy paving pattern is for relatively healthy patients presenting for routine high resolution CT evaluation. In acutely ill patients, the differential diagnosis of these findings is broader

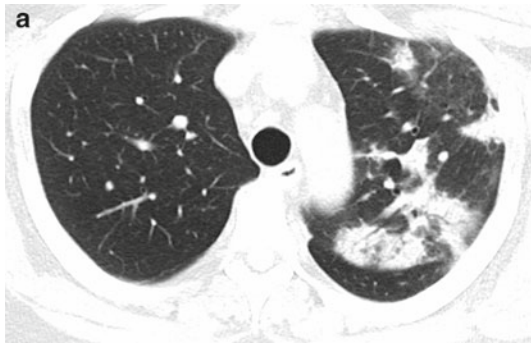


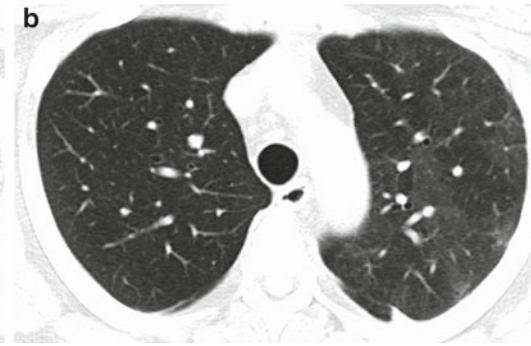


**Fig. 2.2** Consolidation and ground-glass attenuation in a patient with cryptogenic organizing pneumonia. (**a**) Axial CT shows patchy consolidation and some ground-glass attenuation in the left upper lobe. (**b**) CT obtained 3 months later, after steroid treatment, shows resolution of the consolidation, but residual ground-glass attenuation

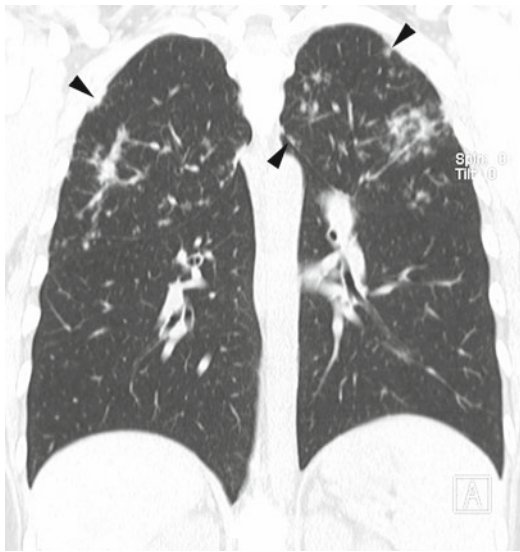

**Fig. 2.3** Perilymphatic nodules in a patient with sarcoidosis. Coronal CT reconstruction shows bilateral upper lung predominant nodules, predominantly clustered along bronchovascular bundles and in the subpleural region (arrowheads)

**Table 2.2** Lobular anatomy in differential diagnosis of infiltrative lung diseases on HRCT

| | |
|---|---|
| Centrilobular nodules: soft tissue attenuation | Pneumoconiosis |
| | Langerhans cell histiocytosis |
| Centrilobular nodules: ground-glass attenuation | Respiratory bronchiolitis |
| | Hypersensitivity pneumonitis |
| Centrilobular nodules with tree-in-bud pattern | Infection |
| | Aspiration |
| | Diffuse panbronchiolitis |
| | Noninfectious bronchiolitis |
| Septal thickening | Left heart failure |
| | Lymphangitic carcinoma |
| | Acute eosinophilic pneumonia |
| | Drug hypersensitivity |
| | Sarcoidosis |

Adapted from Lynch DA. Imaging of diffuse parenchymal lung diseases. In: Schwarz M, King T, editors. Interstitial lung disease. 5th ed. McGraw Hill; 2011. p. 105–49

or pneumoconiosis. Calcific nodules are seen in prior granulomatous infection or in pulmonary alveolar microlithiasis.

## Lines

A variety of linear densities may be seen on HRCT. Thickened interlobular septa (Fig. 2.6) are identified because they are perpendicular to

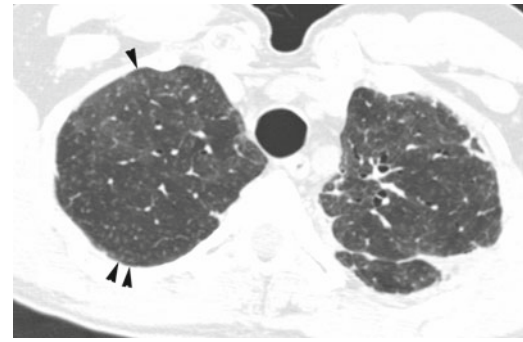

**Fig. 2.4** Centrilobular ground-glass nodules in an individual with hypersensitivity pneumonitis. There are numerous poorly defined centrilobular nodules, most of which are of ground-glass attenuation (i.e., lower in attenuation than the vessels)

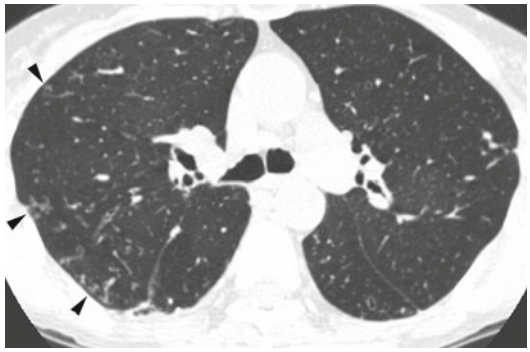

**Fig. 2.5** Tree-in-bud pattern in a patient with nontuberculous mycobacterial infection. Axial CT shows multifocal tree-in-bud pattern in the right lung (arrowheads). There are some centrilobular nodules in the left lung

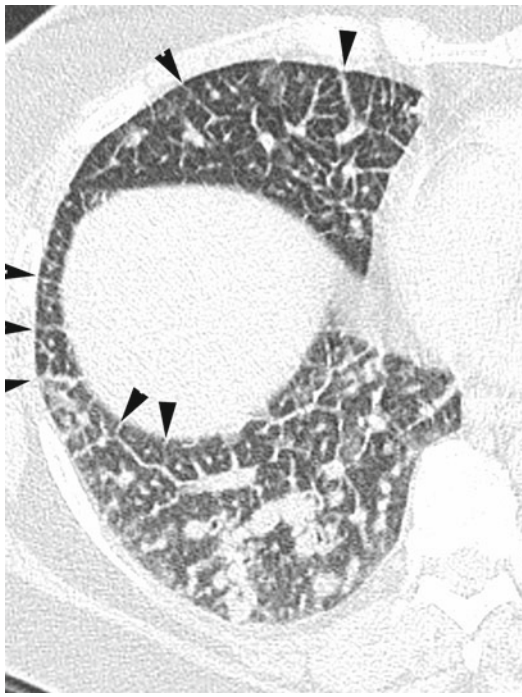

**Fig. 2.6** Interlobular septal thickening in a patient with lymphangitic carcinoma from lung cancer. CT through the right lower lung shows smooth and nodular thickening of numerous interlobular septa, recognized as lines perpendicular to the pleura forming polygonal structures. The bronchovascular bundles are thickened. There is no traction bronchiectasis or architectural distortion to suggest fibrosis

the pleura [7] or by the fact that they form polygonal structures [8]. Reticular lines are probably the commonest type of linear abnormality (Fig. 2.7). These lines are less than 5 mm long, forming a

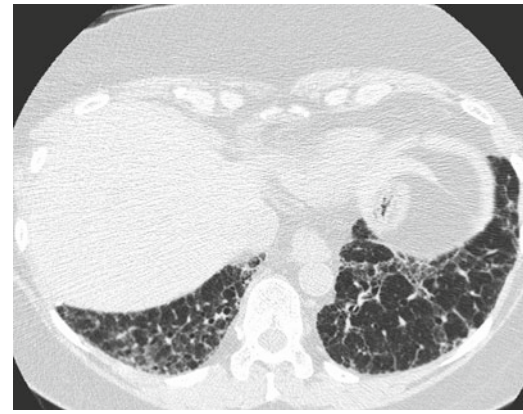

**Fig. 2.7** Reticular pattern in a patient with usual interstitial pneumonia (UIP). Traction bronchiectasis is seen in the right lower lobe. Honeycombing is not present

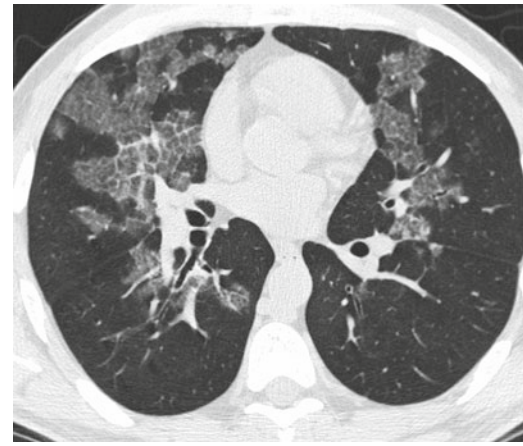

**Fig. 2.8** Crazy paving pattern in a patient with pulmonary alveolar proteinosis. CT through the mid-lungs shows geographic areas of reticular abnormality, formed by thickened interlobular septa and interlobular lines, superimposed on a background of ground-glass attenuation. Traction bronchiectasis and architectural distortion are notably absent. The distribution is predominantly peribronchovascular

fine lace-like network which usually does not conform to lobular anatomy. They are seen in all types of fibrotic lung conditions, particularly idiopathic pulmonary fibrosis [9], collagen vascular disease, and asbestosis. They are usually associated with other evidence of lung fibrosis such as architectural distortion or traction bronchiectasis. Reticular lines are also a prominent CT feature in patients with the crazy paving pattern (Fig. 2.8)

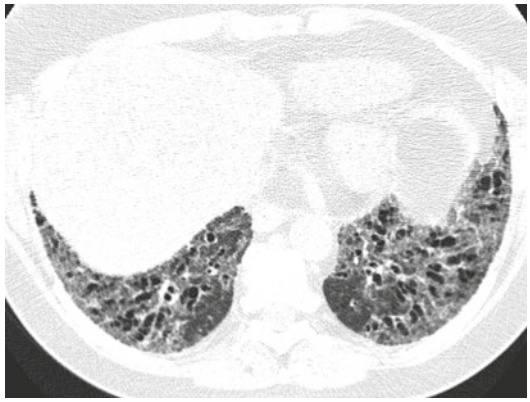

**Fig. 2.9** Traction bronchiectasis in a patient with NSIP. CT shows marked ground-glass attenuation. The associated marked dilation of numerous bronchi indicates that this abnormality is due to fibrosis rather than an inflammatory process

(discussed below), but architectural distortion and traction bronchiectasis are absent.

## Traction Bronchiectasis/ Bronchiolectasis

Traction bronchiectasis and bronchiolectasis (Fig. 2.9) refers to dilatation and distortion of the bronchi and bronchioles in areas of fibrosis, presumed to be due to the forces of increased elastic recoil acting on these structures [10]. It is usually associated with a reticular pattern or with ground-glass attenuation, and is reliable evidence of lung fibrosis [11].

## Honeycombing

Honeycombing is defined as a subpleural cluster or row of cysts (Fig. 2.10). Honeycomb cysts are usually very small (less than 5 mm in diameter). This CT finding correlates with histologic honeycombing and is found in end-stage lung of any cause [12]. Larger honeycomb cysts may sometimes be found in patients with sarcoidosis.

## Cysts

The cysts of interstitial lung disease are air-containing lucencies with a well-defined, complete wall (Fig. 2.11). They are usually round, but may

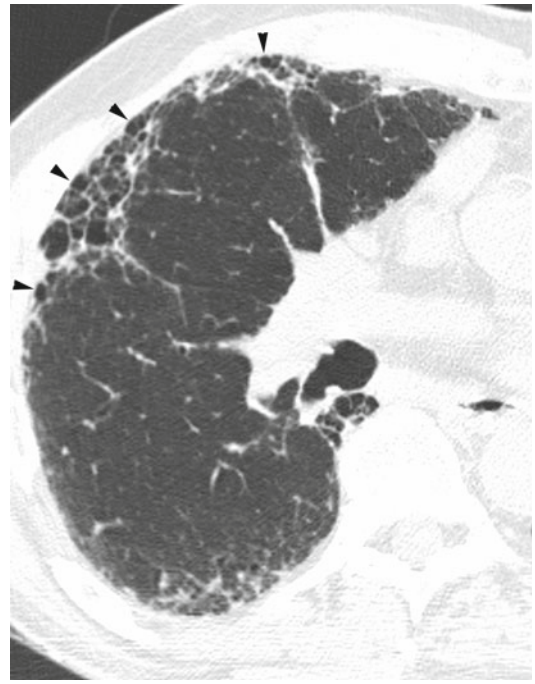

**Fig. 2.10** Honeycombing in a patient with idiopathic pulmonary fibrosis (UIP). Axial CT through the right mid-lung shows clustered subpleural honeycomb cysts (arrowheads)

sometimes be irregular in shape, particularly in Langerhans histiocytosis. They must be distinguished from the "moth-eaten" lucencies of centrilobular emphysema, which are usually irregular in outline and do not have a definable wall (Fig. 2.12). Cysts may be distinguished from bronchiectatic bronchi by the fact that bronchi are usually accompanied by a smaller pulmonary artery, and can usually be traced back to the hilum on serial CT sections.

## Crazy Paving Pattern

The crazy paving pattern is a distinctive pattern characterized by thickened interlobular and intralobular lines forming a geographic network superimposed on a background of ground-glass attenuation (see Fig. 2.8) [13]. In the correct clinical context, this pattern is strongly of pulmonary alveolar proteinosis. Lipoid pneumonia, and, rarely, bronchioloalveolar carcinoma may cause an identical appearance. The pattern can also be

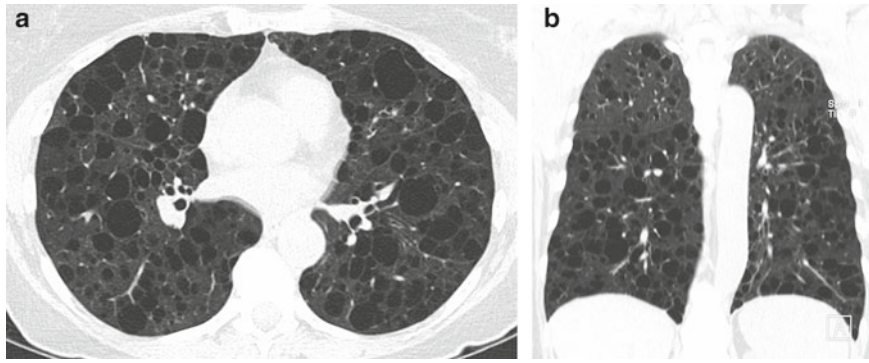


**Fig. 2.11** Pulmonary cysts in a patient with lymphangioleiomyomatosis. (**a**) Axial CT through the mid-lungs shows numerous randomly distributed discrete cysts of varying sizes. Each cyst has a thin, well-defined wall. (**b**) Coronal image shows that distribution in the craniocaudal plane is diffuse

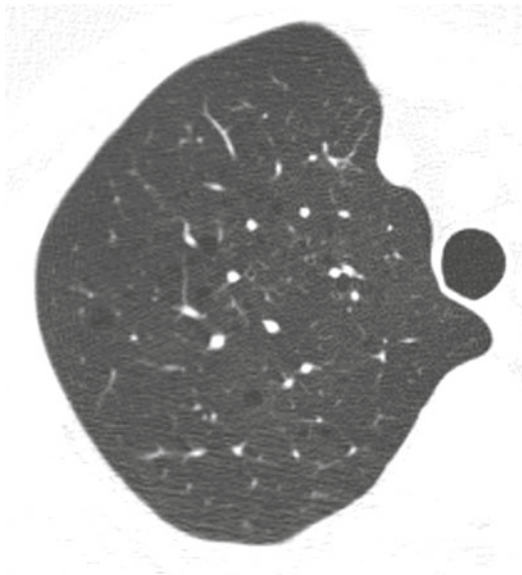

**Fig. 2.12** Centrilobular emphysema. CT through the right upper lung shows well-defined lucencies without a discrete wall

seen in patients with other lung diseases including resolving pneumonia, ARDS, and mucinous bronchioloalveolar carcinoma, but in those conditions it is usually associated with other types of CT abnormality [14–16].

## Decreased Lung Attenuation/Mosaic Pattern

The attenuation (density) of a given area of lung depends on the amount of parenchymal tissue, air, and blood in that area. Therefore, decreased attenuation of the lung may be due to lung destruction (in panlobular emphysema), to decreased blood flow (in vascular disease such as pulmonary thromboembolism), or to decreased ventilation with air trapping and reflex pulmonary oligemia (in small airways diseases with constrictive bronchiolitis) (Fig. 2.13). Panlobular emphysema differs from vascular lung disease and small airway disease in that it usually causes a diffuse decrease in lung attenuation (increased blackness), while thromboembolic disease and obliterative bronchiolitis are commonly (though not always) more patchy in distribution. Vascular disease can often be distinguished from airways disease by comparing inspiratory and expiratory scans. In airways disease, one will expect to see air trapping on the expiratory scans, resulting in an increase in the number of areas of decreased attenuation. In patients with occlusive vascular disease, the areas of decreased attenuation should not increase on expiration [17].

Patients with thromboembolic disease and obliterative bronchiolitis commonly present with a *mosaic pattern*, with lobules of normal attenuation adjacent to lobules or subsegments of decreased attenuation (see Fig. 2.13). A similar mosaic pattern may be caused by parenchymal disease which causes lobular areas of ground-glass attenuation (particularly hypersensitivity pneumonitis) (Fig. 2.14). With the mosaic pattern, it can be difficult to decide whether the abnormal areas are those of decreased attenuation or those of increased attenuation. This distinction can be made by observing the pulmonary

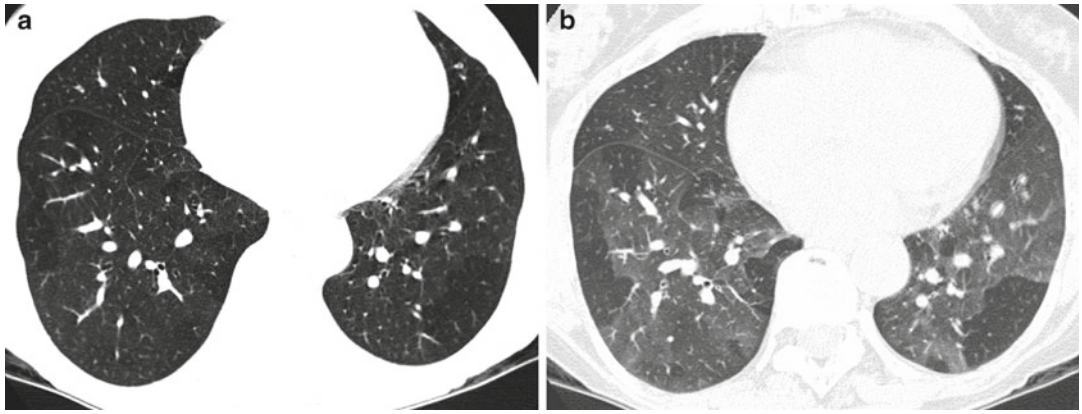


**Fig. 2.13** Mosaic attenuation in a patient with bronchiolitis obliterans related to rheumatoid arthritis. (**a**) Inspiratory CT shows patchy geographic decrease in lung attenuation. Pulmonary vessels are decreased in size in the more lucent parts of lung. (**b**) Expiratory CT confirms that the areas of decreased attenuation on inspiratory images show gas trapping on expiration

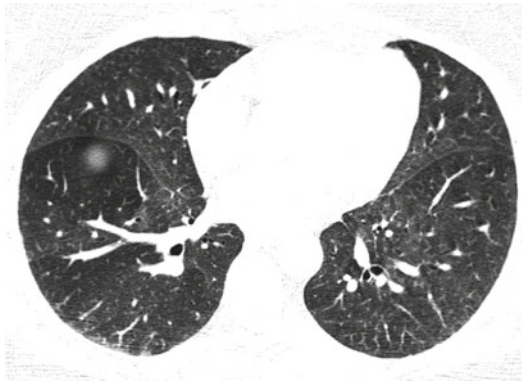

**Fig. 2.14** Mosaic pattern in hypersensitivity pneumonitis. CT through the lower lungs shows diffuse ground-glass abnormality. However, there is focal decreased attenuation in the anterior right lower lobe

vessels, which will be reduced in size in areas affected by vascular occlusive disease or obliterative bronchiolitis, but will be normal in size in patients with parenchymal infiltrative lung diseases [17]. One can then use expiratory images to distinguish between airway obstruction and thromboembolic disease [18]. Of course, physiologic evaluation will also help to distinguish between vascular disease, airways obstruction, and parenchymal infiltration.

## Distribution of Lung Diseases

Evaluation of disease distribution in the craniocaudal and axial planes is remarkably valuable for differential diagnosis of diffuse lung disease (Table 2.3). In the craniocaudal plane, distribution of disease may be characterized as upper lung predominant (Fig. 2.15), lower lung predominant (Fig. 2.16), or (uncommonly) mid-lung predominant. In the axial plane, disease distribution may be characterized as predominantly subpleural or perilymphatic. Perilymphatic abnormalities are usually predominantly distributed along the bronchovascular bundle (where most of the lymphatics of the lung reside), often associated with subpleural nodules and interlobular septal thickening (see Figs. 2.3 and 2.15).

Assessment of the secondary pulmonary lobule may also be valuable in some diffuse diseases (see Table 2.2) [19, 20]. The secondary pulmonary lobule is a basic anatomic and physiologic unit of mammalian lung [21]. In humans, it is an irregularly polyhedral structure composed of several acini, each supplied by a terminal bronchiole. In the center of the secondary pulmonary lobule are the distal bronchus and its terminal bronchioles with the associated distal pulmonary

**Table 2.3** Differential diagnosis of infiltrative lung diseases by distribution within the lung

| | |
|---|---|
| Peripheral distribution | UIP |
| | OP |
| | Asbestosis |
| | Collagen vascular disease |
| | Eosinophilic pneumonia |
| Perilymphatic distribution | Sarcoidosis |
| | Lymphangitic carcinoma |
| | Lymphoproliferative disorders |
| | Organizing pneumonia |
| Upper lobe predominance | Sarcoidosis |
| | Coal workers' pneumoconiosis |
| | Silicosis |
| | Eosinophilic pneumonia |
| | Langerhans cell histiocytosis |
| | Hypersensitivity pneumonitis |
| Lower lobe predominance | UIP |
| | NSIP |
| | OP |
| | Asbestosis |
| | Collagen vascular disease |

*UIP* usual interstitial pneumonia, *OP* organizing pneumonia, *NSIP* nonspecific interstitial pneumonia
Adapted from Lynch DA. Imaging of diffuse parenchymal lung diseases. In: Schwarz M, King T, editors. Interstitial lung disease. 5th ed. McGraw Hill; 2011. p. 105–49

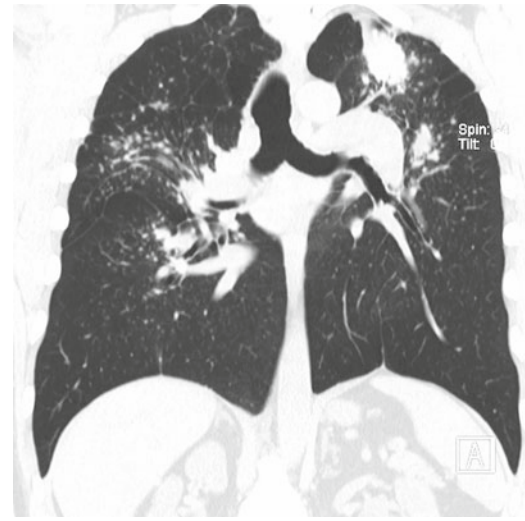

**Fig. 2.15** Upper lung predominant nodules and conglomerate masses in a patient with silicosis. Coronal CT image shows the typical perilymphatic distribution, with predominance of the nodules along bronchovascular bundles, interlobular septa and pleura

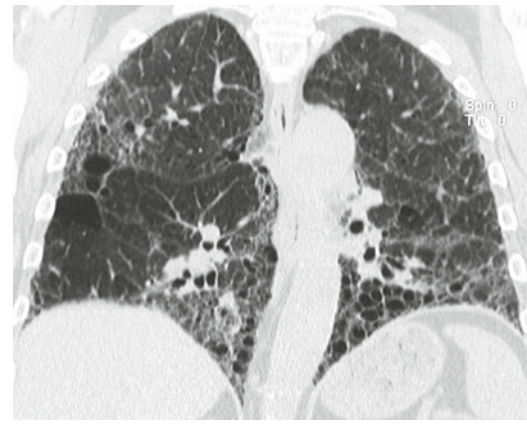

**Fig. 2.16** Lower lung predominant reticular abnormality and honeycombing in a patient with idiopathic pulmonary fibrosis

artery branches. These structures are often called centrilobular or core structures and may be visible on HRCT as a dot or branching structure 1 to 3 mm deep to the pleural surface. In patients with inflammation or plugging of small airways, the normally invisible centrilobular structures become visible as nodules or short branching structures. The centrilobular nodules may either be of soft tissue attenuation or of ground-glass attenuation. When these branching structures terminate in a nodule, the "*tree-in-bud*" sign is present (see Fig. 2.5). The tree-in-bud sign is usually due either to infection or aspiration [22]. Nodules that are centrilobular without a "tree-in-bud" appearance are usually due to some form of inhalational disease (see Fig. 2.4).

The secondary lobules are separated from each other by interlobular septa, which contain branches of the pulmonary veins and lymphatics. On normal HRCT [21], the interlobular septa may be visible in the normal anterior lung as scattered, thin nontapering lines, 1–2 cm long, perpendicular to the pleura and often contacting the pleural surface. Thickening of interlobular

septa is usually due to edema or infiltration of the lymphatic structures, and is often associated with thickening of the other lymphatic pathways (subpleural and peribronchovascular) (see Fig. 2.6).

## Specific Imaging Issues in Evaluation of Diffuse Lung Disease

### Detection of Early Interstitial Lung Disease

The chest radiograph is relatively insensitive for detection of diffuse lung disease. Although it is commonly stated that the chest radiograph is normal in 10–15% of patients with diffuse lung disease, the true sensitivity of the chest radiograph depends on the severity and type of disease present in the population being studied. CT has been shown to be more sensitive than the chest radiograph in many diseases including asbestosis [23], silicosis [24], sarcoidosis [25], scleroderma [26, 27], and hypersensitivity pneumonitis [28, 29]. In asbestosis, HRCT may detect abnormality before resting pulmonary function tests become abnormal [23, 30]. It is also clear that the HRCT scan may be normal despite the presence of biopsy-proven interstitial disease. In a population-based study of subjects with hypersensitivity pneumonitis who had normal resting pulmonary function the sensitivity of HRCT was 38% [31]. Similarly, in a paper by Gamsu and colleagues, CT scanning was normal or near normal in 5 of 25 patients with histologic asbestosis. These studies emphasize the fact that there is a phase in the evolution of any lung disease when the degree of parenchymal infiltration is too slight or too focal to cause a recognizable increase in lung attenuation on CT. Therefore, although CT is substantially more sensitive than the chest radiograph for ILD, normal findings on HRCT cannot be used to exclude ILD. In future, it is possible that computer-based characterization systems might help to detect lung disease in patients with visually normal CT.

### Characterization of Interstitial Lung Disease

Several large retrospective studies have compared the diagnostic accuracy of chest CT and chest radiography for diagnosis of specific lung diseases. Mathieson et al. [32] examined the chest radiographs and CT scans of 118 patients with diffuse infiltrative lung diseases. For usual interstitial pneumonitis, the first choice diagnosis was correct in 75% of the cases on chest radiograph and 89% of the cases on CT. For silicosis, the corresponding figures were 63 and 93%, and sarcoidosis, 61 and 77%. For lymphangitic carcinomatosis, the first choice diagnosis was correct in 56% of cases on the chest radiograph and 85% on CT. In addition, interobserver variation appeared to be less for CT scanning than for chest radiographs. Overall, a correct first choice diagnosis was made with 57% of radiographs and 76% of CT scans.

One of the defects of these earlier studies was that they may have included patients with well-established disease. In a more recent study of 85 patients who were scanned prior to surgical lung biopsy, the accuracy of a confident first choice diagnosis of disease was 90%, but such a confident diagnosis was made in only about 25% of cases [33]. This relatively low level of diagnostic confidence was most likely due to selection bias (patients in whom confident CT diagnoses can be made are unlikely to undergo biopsy). However, it is also possible that confident diagnoses are more difficult to make in those with earlier disease.

A prospective, multicenter study of the accuracy of diagnosis of usual interstitial pneumonia (UIP) found that a confident CT diagnosis of UIP, based on typical features, was correct in 96% of cases [34], consistent with the results of several other studies indicating that the correctness of a confident first choice diagnosis of UIP, made by an experienced radiologist, is greater than 90% [33, 35, 36]. Univariate and multivariate analysis showed that radiologic features were the primary discriminants between UIP and other causes of diffuse lung disease [37]. However, it should be noted that in this study, a confident CT diagnosis

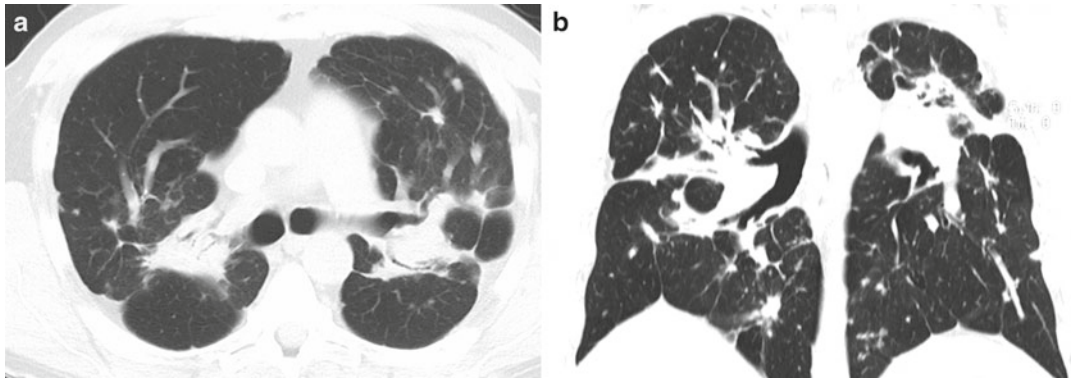


**Fig. 2.17** Fibrotic sarcoidosis. Axial (**a**) and coronal (**b**) CT reconstructions demonstrate upper lobe predominant perihilar conglomerate masses associated with marked bronchovascular distortion

of UIP was made in only about 50% of cases. In other cases of histologically confirmed UIP, the CT features were not typical enough to make a confident diagnosis. Similar findings were reported in a study by Raghu et al. [38]. Other diseases in which a confident CT diagnosis is highly likely to be correct include lymphangitic carcinoma [8], Langerhans histiocytosis [39], lymphangiomyomatosis [39], and hypersensitivity pneumonitis (with micronodules) [40]. Advanced cases of sarcoidosis may also be diagnosed with confidence (see Fig. 2.17).

It must be clearly understood that even a confident CT diagnosis should be integrated with the available clinical information. Patients with discrepant findings on clinical evaluation and CT should usually undergo biopsy. Biopsy is also indicated in patients with nonspecific CT findings. HRCT can be valuable for predicting whether transbronchial biopsy would be helpful (in suspected sarcoidosis or lymphangitic carcinoma), and for identifying a suitable site for biopsy by the bronchoscopist or surgeon. When a biopsy is performed, it is important to review the biopsy in conjunction with the CT findings. Discrepancies between the CT pattern and the biopsy findings may be due to sampling of a nonrepresentative part of the lung.

## CT of Specific Lung Diseases

### Idiopathic Interstitial Pneumonias

UIP often has a characteristic appearance on CT [41]. The predominant CT pattern is usually either reticular abnormality, almost always associated with traction bronchiectasis, and frequently associated with honeycombing (see Figs. 2.7, 2.10, and 2.16) [42]. Pure ground-glass attenuation, if present, is usually sparse. The distribution of the abnormalities is basal predominant in most, but may be diffuse in the craniocaudal plane. Peripheral, subpleural predominance is present in over 90%. The fibrosis is asymmetric in up to 25% of cases [43]. In contrast to the homogenous appearance of nonspecific interstitial pneumonia (NSIP), the abnormalities of UIP often have a patchy distribution. As the disease progresses, it often appears to "creep" up the periphery of the lung, causing subpleural reticular abnormality in the upper lungs [37].

Multiple prospective and retrospective studies have shown that a confident or highly confident diagnosis of UIP, based on the CT features outlined earlier, has a specificity of over 90% for the pathologic diagnosis of UIP [33–35, 38, 40, 42]. Honeycombing in the lower lobes, and linear

abnormality in the upper lobes, are the most reliable features for differentiating between UIP and its clinical mimics (see Fig. 2.10) [37]. In a study by Flaherty et al., the observation of honeycombing on HRCT indicated the presence of UIP with a sensitivity of 90% and specificity of 86% [44]. However, there is a substantial minority (30–50%) of cases with histologic UIP (without honeycombing) in whom a confident diagnosis of UIP cannot be made based on the CT appearances (see Fig. 2.7). In these patients, the CT appearances of UIP overlap with those of NSIP and chronic hypersensitivity pneumonitis, and the diagnosis can only be established by lung biopsy.

Published descriptions of the CT appearances of NSIP have varied quite widely [42, 45–52], probably because of differing pathologic diagnostic criteria. However, a multidisciplinary workshop identified a relatively typical CT appearance among 67 patients who received a clinical–radiologic–pathologic consensus diagnosis of NSIP [53]. In this group, the CT appearances were characterized by confluent, symmetric, basal predominant, ground-glass and reticular abnormality with traction bronchiectasis and lower lobe volume loss (see Fig. 2.9). In contrast to UIP, the subpleural lung is often spared.

Consolidation is the radiologic hallmark of cryptogenic organizing pneumonia, seen in about 80% of cases (see Fig. 2.2). It generally shows no craniocaudal predilection though some series have shown a basal predominance [54–56]. The consolidation may have a perilymphatic distribution [57–61]. Other suggestive features may include a perilobular pattern (poorly defined opacity along interlobular septa) and the reverse halo sign (ring-like opacity with central ground-glass abnormality) [62, 63].

Lymphoid interstitial pneumonia is characterized by ground-glass abnormality. Discrete cysts may be seen in two-thirds of cases [64], and may be the dominant or only finding. The cysts typically have a perilymphatic distribution and usually lower lung predominant. Mediastinal or hilar lymphadenopathy is often seen.

**Table 2.4** Patterns of lung injury most commonly associated with specific collagen vascular diseases

| Disease entity | Lung pattern |
|---|---|
| Diffuse scleroderma | Nonspecific interstitial pneumonia |
| | Pulmonary hypertension |
| Limited scleroderma | Pulmonary hypertension |
| Rheumatoid arthritis | Usual interstitial pneumonia |
| | Obliterative bronchiolitis |
| | Follicular bronchiolitis |
| Polymyositis/ dermatomyositis | Nonspecific interstitial pneumonia |
| | Organizing pneumonia |
| Sjögren's syndrome | LIP |
| | Follicular bronchiolitis |
| Systemic lupus erythematosus | Pulmonary hemorrhage |

## Collagen Vascular Disease

Involvement of the respiratory system in the collagen vascular diseases is common. Most of the parenchymal manifestations of collagen vascular disease are similar to those found in idiopathic interstitial pneumonias [65] and can be classified using the same system [66]. Although any pattern of lung injury may occur with any of the collagen vascular diseases, each specific collagen vascular disease tends to be associated with two or three specific patterns of injury, summarized in Table 2.4.

## Sarcoidosis

The manifestations of sarcoidosis in the lung are diverse. However, the salient features are lymphadenopathy and nodules. Hilar and mediastinal lymphadenopathy is typically symmetric and may be partially calcified. The nodules are characteristically clustered in a perilymphatic distribution (see Fig. 2.3) [5], and often regress at least partially with treatment. Other potentially reversible findings in sarcoidosis include large nodular opacities,

septal thickening ground-glass abnormality, and consolidation [67].

In fibrotic sarcoidosis, perihilar clustered nodules form conglomerate masses, associated with bronchovascular distortion (Fig. 2.17) [68]. While the size of these fibrotic masses may decrease with time, the associated bronchial distortion usually persists or increases. Honeycombing may also be seen [69].

## Hypersensitivity Pneumonitis

Hypersensitivity pneumonitis may be diagnosed on CT with high confidence in the presence of either of the following findings:

- Profuse, diffuse, poorly defined centrilobular nodules of ground-glass attenuation (see Fig. 2.4).
- Ground-glass attenuation associated with widespread multilobular decreased lung attenuation and expiratory air trapping (see Fig. 2.14).

A proportion of subjects with chronic hypersensitivity pneumonitis have lung fibrosis, which may be difficult to distinguish from UIP or NSIP. Features that help to distinguish chronic fibrotic HP from UIP and NSIP include upper or mid-lung predominance, sparing of the extreme lung bases, and the presence of multiple lobules of decreased attenuation and air trapping [36, 70].

## Smoking-Related Lung Diseases

Infiltrative lung diseases caused by cigarette smoking include respiratory bronchiolitis, respiratory bronchiolitis-interstitial lung disease, desquamative interstitial pneumonia, and pulmonary Langerhans cell histiocytosis (PLCH). On CT scanning, patients with asymptomatic respiratory bronchiolitis generally show mild centrilobular nodularity and small patches of ground-glass attenuation [71].

In RB-ILD, centrilobular nodularity and ground-glass attenuation are usually more extensive than in asymptomatic RB (Fig. 2.18) [72]. Emphysema, bronchial wall thickening, and areas of decreased lung attenuation are commonly also present [73]. When patchy abnormalities of this type are present in heavy smokers with impaired pulmonary function, RB-ILD may be diagnosed with a high degree of confidence. The CT findings of RB-ILD are at least partially reversible in patients who stop smoking [73, 74].

Ground-glass attenuation is seen in all pati ents with DIP [46], with lower lobe predominance in about 75% of the patients (Fig. 2.19). Peripheral predominance is seen in about 60%.

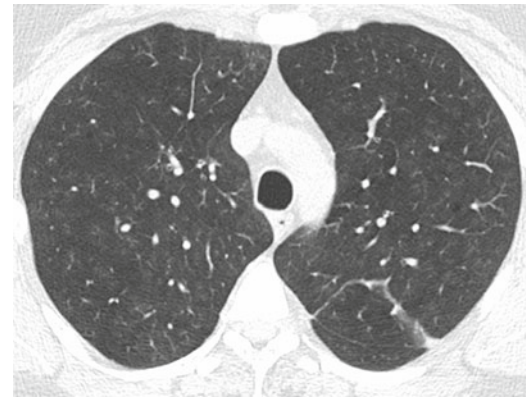

**Fig. 2.18** Respiratory bronchiolitis interstitial lung disease in a patient with a 38 pack-year history of cigarette smoking. CT through the upper lungs shows marked airway wall thickening, with widespread poorly defined ground-glass attenuation, and smudgy centrilobular nodularity

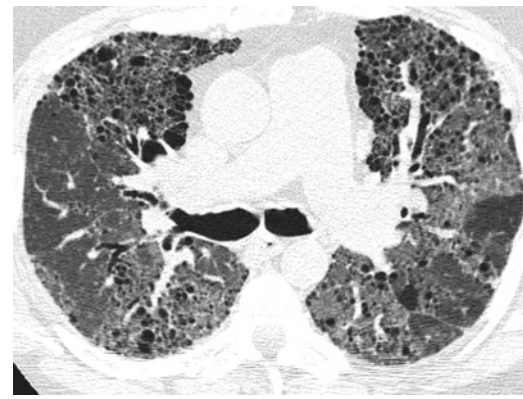

**Fig. 2.19** Desquamative interstitial pneumonia in a cigarette smoker. CT through the mid-lungs shows diffuse ground-glass attenuation. Numerous cysts are seen within the areas of ground glass. In contrast to honeycomb cysts, these cysts do not show subpleural clustering

Cysts are seen within areas of ground-glass attenuation in at least 50% of cases (Fig. 2.19).

## Cystic Lung Diseases

The most common cystic lung diseases are PLCH, lymphangioleiomyomatosis (LAM), and lymphoid interstitial pneumonia. The combination of pulmonary nodules and cysts, predominating in the upper lungs is virtually diagnostic of PLCH (Fig. 2.20) [75–78]. The nodules may be well defined, poorly defined, or stellate, and may be cavitary. The cysts are often irregular or lobulated in outline. PLCH may be distinguished from LAM by the presence of nodules, by the irregular outline of the cysts, and by the sparing of the lung bases.

Cysts are the pathognomonic feature of LAM (see Fig. 2.11) [79–85]. The cysts are usually multiple and distributed in a uniform fashion in lung that is otherwise normal. Cysts are clearly demarcated by a thin even wall (1–2 mm thick) and are usually rounded. Vessels are often seen at the margins of the cysts. The cysts are usually 5–15 mm, but may range from 2 to 50 mm. The number of cysts varies widely, depending on the clinical presentation; cysts are usually extensive in those who present with symptoms of pulmonary impairment, but often quite sparse in those who present with complications such as pneumothorax, pleural effusion, etc. CT has enhanced awareness of the intra-abdominal manifestations of LAM. In addition to renal angiomyolipomas (found in 30–50% of patients), other manifestations include hepatic angiomyolipomas, lymphangiomyomas, and enlarged retroperitoneal lymph nodes [86, 87].

Cysts are often a salient feature of LIP, discussed earlier. The predominantly perilymphatic distribution of these cysts usually helps distinguish them from LAM and PLCH.

**Fig. 2.20** Pulmonary Langerhans cell histiocytosis in a young cigarette smoker. Coronal CT shows poorly defined centrilobular nodules in the upper lungs associated with a few small cysts. The associated ground-glass attenuation may represent a component of respiratory bronchiolitis interstitial lung disease

## Small Airways Disease

Computed tomography has contributed substantially to our understanding of small airways diseases and offers a convenient method for classification of these diverse entities. A current CT-based classification of small airways disease is presented in Table 2.5.

In patients with constrictive bronchiolitis (see Fig. 2.13), the primary CT finding is dramatic decrease in lung density in affected lobules or subsegments, associated with narrowing of the pulmonary vessels. Such findings are identified in individuals with obliterative bronchiolitis related to prior infection, connective tissue disease, toxic fume inhalation, and transplantation [88–92]. Expiratory images are usually helpful in confirming air trapping.

Cellular bronchiolitis is characterized on CT by centrilobular nodularity with a tree-in-bud pattern (see Fig. 2.5). It is most commonly seen in patients with acute or chronic pulmonary infection. In the acute context, it is usually seen in patients with atypical pneumonia due to mycoplasma [93] or viruses. In those who are not acutely ill, the most common causes are mycobacterial infection and aspiration.

**Table 2.5** CT-based classification of small airways diseases

| Radiologic pattern | Characteristic radiologic features | Causes |
|---|---|---|
| Cellular bronchiolitis | Centrilobular nodularity | Acute or chronic infection (mycobacterial, fungal) |
| | Tree-in-bud pattern | Aspiration |
| | | Hypersensitivity pneumonitis |
| Constrictive bronchiolitis | Diffuse or geographic air trapping/ mosaic pattern | Rheumatoid disease |
| | Bronchial dilation | Chronic rejection |
| | | Childhood viral/mycoplasma infection |
| | | Prior toxic fume exposure |
| | | Cryptogenic bronchiolitis obliterans |
| Panbronchiolitis | Tree-in-bud pattern | Diffuse panbronchiolitis |
| | Bronchiolectasis | Cystic fibrosis |
| | Bronchiectasis | Immune deficiency |
| | | Nontuberculous mycobacterial infection |
| | | Inflammatory bowel disease |
| Respiratory bronchiolitis | Poorly defined centrilobular nodules | Other inhalation exposures |
| | Patchy ground-glass attenuation | |
| Follicular bronchiolitis | Centrilobular nodules | Sjogren syndrome and other collagen vascular diseases |
| | Peribronchial nodules | Immunodeficiency |
| | Ground-glass opacity | |

Adapted from Lynch DA. Imaging of diffuse parenchymal lung diseases. In: Schwarz M, King T, editors. Interstitial lung disease. 5th ed. McGraw Hill; 2011. p. 105–49

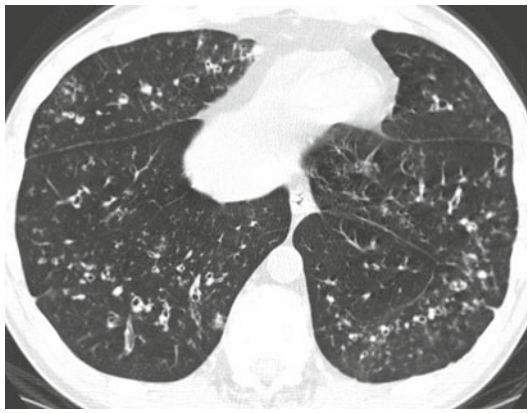

**Fig. 2.21** Diffuse panbronchiolitis pattern in a patient with ulcerative colitis. CT through the lower lungs shows widespread cylindric bronchiectasis and multifocal tree-in-bud pattern. Differential diagnosis would include chronic infection

Panbronchiolitis, typically seen in Asian patients, is associated with tree-in-bud pattern associated with bronchiolar dilation, bronchiectasis, and patchy consolidation [94]. The abnormality is usually most marked in the lower lobes bilaterally. A similar pattern may be seen in individuals with inflammatory bowel disease (see Fig. 2.21).

## CT-Based Strategy for Diagnosis of Diffuse Lung Disease

HRCT is now a pivotal modality in establishing the diagnosis of diffuse lung disease. Table 2.6 presents a proposed strategy for this purpose. A few points are important with regard to this table:

- The level of diagnostic confidence of the radiologic diagnosis is very important and should be specifically stated. A high-confidence diagnosis, based on typical features, is much more likely to be correct than a lower confidence diagnosis, particularly with IPF.
- Certain radiologic findings, particularly ground-glass abnormality, consolidation, and reticular abnormality are relatively nonspecific and will usually require further diagnostic evaluation.

**Table 2.6** Diagnostic strategy in diffuse lung disease based on CT features

| |
|---|
| *Category 1: No invasive procedures needed if clinical and CT features are typical* |
| Usual interstitial pneumonia |
| Lymphangiomyomatosis |
| Langerhans histiocytosis |
| Hypersensitivity pneumonitis |
| Pneumoconiosis |
| Collagen vascular disease |
| *Category 2: Bronchoalveolar lavage* |
| Pulmonary alveolar proteinosis |
| Infection |
| *Category 3: Transbronchial biopsy* |
| Sarcoid |
| Lymphangitic carcinoma |
| Lymphoproliferative disorders |
| *Category 4: Surgical lung biopsy* |
| Nonspecific CT appearances (e.g., ground-glass abnormality, reticular abnormality), without a clinical explanation |
| Typical CT appearance of a condition, with atypical clinical features |
| Typical clinical features of a condition, with atypical CT |

Adapted from Lynch DA. Imaging of diffuse parenchymal lung diseases. In: Schwarz M, King T, editors. Interstitial lung disease. 5th ed. McGraw Hill; 2011. p. 105–49

- CT may be helpful in identifying optimal sites for transbronchial or surgical biopsy.
- If clinical or imaging features are atypical, biopsy is still indicated.

## References


1. Mayo JR. CT evaluation of diffuse infiltrative lung disease: dose considerations and optimal technique. J Thorac Imaging. 2009;24(4):252–9.
2. Hansell DM, Bankier AA, Macmahon H, McLoud TC, Müller NL, Remy J. Fleischner Society: glossary of terms for thoracic imaging. Radiology. 2008; 246(3):697–722.
3. Leung A, Miller R, Müller N. Parenchymal opacification in chronic infiltrative lung disease: CT-pathologic correlation. Radiology. 1993;188:209–14.
4. Austin J, Müller N, Friedman P, Hansell D, Naidich D, Remy-Jardin M, et al. Glossary of terms for CT of the lungs: recommendations of the nomenclature committee of the Fleischner Society. Radiology. 1996;200:327–31.
5. Remy-Jardin M, Beuscart R, Sault MC, Marquette CH, Remy J. Subpleural micronodules in diffuse infiltrative lung diseases: evaluation with thin-section CT scans. Radiology. 1990;177(1):133–9.
6. Gruden JF, Webb WR, Naidich DP, McGuinness G. Multinodular disease: anatomic localization at thin-section CT – multireader evaluation of a simple algorithm. Radiology. 1999;210(3):711–20.
7. Aberle DR, Gamsu G, Ray CS, Feuerstein IM. Asbestos-related pleural and parenchymal fibrosis: detection with high-resolution CT. Radiology. 1988;166:729–34.
8. Stein M, Mayo J, Müller N, Aberle D, Webb W, Gamsu G. Pulmonary lymphangitic spread of carcinoma: appearance on CT scans. Radiology. 1987; 162:371–5.
9. Müller NL, Miller RR, Webb WR, Evans KG, Ostrow DN. Fibrosing alveolitis: CT-pathologic correlation. Radiology. 1986;160(3):585–8.
10. Westcott JL, Cole SR. Traction bronchiectasis in end-stage pulmonary fibrosis. Radiology. 1986;161: 665–9.
11. Remy-Jardin M, Giraud F, Remy J, Copin MC, Gosselin B, Duhamel A. Importance of ground-glass attenuation in chronic diffuse infiltrative lung disease: pathologic-CT correlation. Radiology. 1993;189(3):693–8.
12. Meziane MA, Hruban RH, Zerhouni EA, Wheeler PS, Khouri NF, Fishman EK, et al. High resolution CT of the lung parenchyma with pathologic correlation. Radiographics. 1988;8(1):27–54.
13. Godwin J, Müller N, Takasugi J. Pulmonary alveolar proteinosis: CT findings. Radiology. 1988;169:609–13.
14. Tan RT, Kuzo RS. High-resolution CT findings of mucinous bronchioloalveolar carcinoma: a case of pseudopulmonary alveolar proteinosis. AJR Am J Roentgenol. 1997;168(1):99–100.
15. Laurent F, Philippe JC, Vergier B, Granger-Veron B, Darpeix B, Vergeret J, et al. Exogenous lipoid pneumonia: HRCT, MR, and pathologic findings. Eur Radiol. 1999;9(6):1190–6.
16. Murayama S, Murakami J, Yabuuchi H, Soeda H, Masuda K. "Crazy paving appearance" on high resolution CT in various diseases. J Comput Assist Tomogr. 1999;23(5):749–52.
17. Stern E, Swensen S, Hartman T, Frank M. CT mosaic pattern of lung attenuation: distinguishing different causes. AJR Am J Roentgenol. 1995;165:813–6.
18. Arakawa H, Webb WR, McCowin M, Katsou G, Lee KN, Seitz RF. Inhomogeneous lung attenuation at thin-section CT: diagnostic value of expiratory scans. Radiology. 1998;206(1):89–94.
19. Murata K, Khan A, Herman PG. Pulmonary parenchymal disease: evaluation with high-resolution CT. Radiology. 1989;170:629–35.
20. Noma S, Khan A, Herman PG, Rojas KA. High-resolution computed tomography of the pulmonary parenchyma. Semin Ultrasound CT MR. 1990;11: 365–79.
21. Webb W, Stein M, Finkbeiner W, Im J-G, Lynch D, Gamsu G. Normal and diseased isolated lungs: high resolution CT. Radiology. 1988;166:81–7.
22. Murata K, Itoh H, Todo G, Kanaoka M, Noma S, Itoh T, et al. Centrilobular lesions of the lungs: demonstration

by high-resolution CT and pathologic correlation. Radiology. 1986;161:641–5.
23. Staples CA, Gamsu G, Ray CS, Webb WR. High resolution computed tomography and lung function in asbestos-exposed workers with normal chest radiographs. Am Rev Respir Dis. 1989;139:1502–8.
24. Begin R, Ostiguy G, Fillion R, Colman N. Computed tomography in the early detection of silicosis. Am Rev Respir Dis. 1991;144:697–705.
25. Bergin C, Bell D, Coblentz C, et al. Sarcoidosis: correlation of pulmonary parenchymal pattern at CT with results of pulmonary function tests. Radiology. 1989;171:619–24.
26. Harrison NK, Glanville AR, Strickland B, Haslam PL, Corrin B, Addis BJ, et al. Pulmonary involvement in systemic sclerosis: the detection of early changes by thin section CT scan, bronchoalveolar lavage and 99mTc-DTPA clearance. Respir Med. 1989;83(5):403–14.
27. Schurawitzki H, Stiglbauer R, Graninger W, Herold C, Polzleitner D, Burghuber OC, et al. Interstitial lung disease in progressive systemic sclerosis: high-resolution CT versus radiography. Radiology. 1990;176(3):755–9.
28. Hansell D, Moskovic E. High-resolution computed tomography in extrinsic allergic alveolitis. Clin Radiol. 1991;43:8–12.
29. Silver S, Müller N, Miller R, Lefcoe M. Hypersen sitivity pneumonitis: evaluation with CT. Radiology. 1989;173:441–5.
30. Aberle DR, Gamsu G, Ray CS. High-resolution CT of benign asbestos-related diseases: clinical and radiographic correlation. AJR Am J Roentgenol. 1988; 151(5):883–91.
31. Lynch DA, Rose CS, Way D, King TJ. Hypersensitivity pneumonitis: sensitivity of high-resolution CT in a population-based study. Am J Roentgenol. 1992;159: 469–72.
32. Mathieson JR, Mayo JR, Staples CA, Müller NL. Chronic diffuse infiltrative lung disease: comparison of diagnostic accuracy of CT and chest radiography. Radiology. 1989;171(1):111–6.
33. Swensen S, Aughenbaugh G, Myers J. Diffuse lung disease: diagnostic accuracy of CT in patients undergoing surgical biopsy of the lung. Radiology. 1997; 205:229–34.
34. Hunninghake GW, Zimmerman MB, Schwartz DA, King TE, Lynch J, Hegele R, et al. Utility of a lung biopsy for the diagnosis of idiopathic pulmonary fibrosis. Am J Respir Crit Care Med. 2001;164(2):193–6.
35. Tung KT, Wells AU, Rubens MB, Kirk JM, du Bois RM, Hansell DM. Accuracy of the typical computed tomographic appearances of fibrosing alveolitis. Thorax. 1993;48(4):334–8.
36. Lynch D, Newell J, Logan P, King T, Müller N. Can CT distinguish idiopathic pulmonary fibrosis from hypersensitivity pneumonitis? AJR Am J Roentgenol. 1995;165:807–11.
37. Hunninghake GW, Lynch DA, Galvin JR, Gross BH, Müller N, Schwartz DA, et al. Radiologic findings are strongly associated with a pathologic diagnosis of usual interstitial pneumonia. Chest. 2003;124(4):1215–23.
38. Raghu G, Mageto YN, Lockhart D, Schmidt RA, Wood DE, Godwin JD. The accuracy of the clinical diagnosis of new-onset idiopathic pulmonary fibrosis and other interstitial lung disease: a prospective study. Chest. 1999;116(5):1168–74.
39. Bonelli FS, Hartman TE, Swensen SJ, Sherrick A. Accuracy of high-resolution CT in diagnosing lung diseases. AJR Am J Roentgenol. 1998;170(6):1507–12.
40. Nishimura K, Izumi T, Kitaichi M, Nagai S, Itoh H. The diagnostic accuracy of high-resolution computed tomography in diffuse infiltrative lung diseases. Chest. 1993;104(4):1149–55.
41. Sumikawa H, Johkoh T, Ichikado K, Taniguchi H, Kondoh Y, Fujimoto K, et al. Usual interstitial pneumonia and chronic idiopathic interstitial pneumonia: analysis of CT appearance in 92 patients. Radiology. 2006;241(1):258–66.
42. Johkoh T, Müller NL, Cartier Y, Kavanagh PV, Hartman TE, Akira M, et al. Idiopathic interstitial pneumonias: diagnostic accuracy of thin-section CT in 129 patients. Radiology. 1999;211(2):555–60.
43. Sumikawa H, Johkoh T, Colby TV, Ichikado K, Suga M, Taniguchi H, et al. Computed tomography findings in pathological usual interstitial pneumonia: relationship to survival. Am J Respir Crit Care Med. 2008; 177(4):433–9.
44. Flaherty KR, Toews GB, Travis WD, Colby TV, Kazerooni EA, Gross BH, et al. Clinical significance of histological classification of idiopathic interstitial pneumonia. Eur Respir J. 2002;19(2):275–83.
45. Kim EY, Lee KS, Chung MP, Kwon OJ, Kim TS, Hwang JH. Nonspecific interstitial pneumonia with fibrosis: serial high-resolution CT findings with functional correlation. AJR Am J Roentgenol. 1999; 173(4):949–53.
46. Hartman TE, Primack SL, Swensen SJ, Hansell D, McGuinness G, Müller NL. Desquamative interstitial pneumonia: thin-section CT findings in 22 patients. Radiology. 1993;187(3):787–90.
47. Park JS, Lee KS, Kim JS, Park CS, Suh YL, Choi DL, et al. Nonspecific interstitial pneumonia with fibrosis: radiographic and CT findings in seven patients. Radiology. 1995;195(3):645–8.
48. Cottin V, Donsbeck A, Revel D, Loire R, Cordier J. Nonspecific interstitial pneumonia: individualization of a clinicopathologic entity in a series of 12 patients. Am J Respir Crit Care Med. 1998;158:1286–93.
49. Nagai S, Kitaichi M, Itoh H, Nishimura K, Izumi T, Colby TV. Idiopathic nonspecific interstitial pneumonia/fibrosis: comparison with idiopathic pulmonary fibrosis and BOOP. Eur Respir J. 1998;12(5):1010–9.
50. Johkoh T, Müller NL, Colby TV, Ichikado K, Taniguchi H, Kondoh Y, et al. Nonspecific interstitial pneumonia: correlation between thin-section CT findings and pathologic subgroups in 55 patients. Radiology. 2002;225(1):199–204.
51. Nishiyama O, Kondoh Y, Taniguchi H, Yamaki K, Suzuki R, Yokoi T, et al. Serial high resolution CT findings in nonspecific interstitial pneumonia/fibrosis. J Comput Assist Tomogr. 2000;24(1):41–6.

52. MacDonald S, Rubens M, Hansell D, Copley S, Desai S, du Bois R, et al. Nonspecific interstitial pneumonia and usual interstitial pneumonia: comparative appearances and diagnostic accuracy of high-resolution computed tomography. Radiology. 2001;221:600–5.
53. Travis WD, Hunninghake G, King Jr TE, Lynch DA, Colby TV, Galvin JR, et al. Idiopathic nonspecific interstitial pneumonia: report of an American Thoracic Society project. Am J Respir Crit Care Med. 2008; 177(12):1338–47.
54. Epler GR, Colby TV, McLoud TC, Gaensler EA, Carrington CB. Bronchiolitis obliterans organizing pneumonia. N Engl J Med. 1985;312(3):152–8.
55. Costabel U, Teschler H, Schoenfeld B, Hartung W, Nusch A, Guzman J, et al. BOOP in Europe. Chest. 1992;102(1 Suppl):14S–20S.
56. Izumi T, Kitaichi M, Nishimura K, Nagai S. Bronchiolitis obliterans organizing pneumonia. Clinical features and differential diagnosis. Chest. 1992;102(3):715–9.
57. Müller NL, Colby TV. Idiopathic interstitial pneumonias: high-resolution CT and histologic findings. Radiographics. 1997;17(4):1016–22.
58. Alasaly K, Müller N, Ostrow DN, Champion P, FitzGerald JM. Cryptogenic organizing pneumonia. A report of 25 cases and a review of the literature. Medicine. 1995;74(4):201–11.
59. Haddock JA, Hansell DM. The radiology and terminology of cryptogenic organizing pneumonia. Br J Radiol. 1992;65(776):674–80.
60. Bartter T, Irwin RS, Nash G, Balikian JP, Hollingsworth HH. Idiopathic bronchiolitis obliterans organizing pneumonia with peripheral infiltrates on chest roentgenogram. Arch Intern Med. 1989;149(2):273–9.
61. Müller NL, Staples CA, Miller RR. Bronchiolitis obliterans organizing pneumonia: CT features in 14 patients. AJR Am J Roentgenol. 1990;154:983–7.
62. Kim SJ, Lee KS, Ryu YH, Yoon YC, Choe KO, Kim TS, et al. Reversed halo sign on high-resolution CT of cryptogenic organizing pneumonia: diagnostic implications. AJR Am J Roentgenol. 2003;180(5):1251–4.
63. Polverosi R, Maffesanti M, Dalpiaz G. Organizing pneumonia: typical and atypical HRCT patterns. Radiol Med. 2006;111(2):202–12.
64. Johkoh T, Müller NL, Pickford HA, Hartman TE, Ichikado K, Akira M, et al. Lymphocytic interstitial pneumonia: thin-section CT findings in 22 patients. Radiology. 1999;212(2):567–72.
65. American Thoracic Society/European Respiratory Society international multidisciplinary consensus classification of the idiopathic interstitial pneumonias. Am J Respir Crit Care Med. 2002;165(2):277–304.
66. Kim EA, Lee KS, Johkoh T, Kim TS, Suh GY, Kwon OJ, et al. Interstitial lung diseases associated with collagen vascular diseases: radiologic and histopathologic findings. Radiographics. 2002;22(Spec No):S151–65.
67. Murdoch J, Müller N. Pulmonary sarcoidosis: changes on followup examination. Am J Roentgenol. 1992; 159:473–7.
68. Brauner M, Grenier P, Mompoint D, Lenoir S, deCremoux HP. Pulmonary sarcoidosis: evaluation with high resolution CT. Radiology. 1989;172:467–71.
69. Hennebicque AS, Nunes H, Brillet PY, Moulahi H, Valeyre D, Brauner MW. CT findings in severe thoracic sarcoidosis. Eur Radiol. 2005;15(1):23–30.
70. Silva CI, Müller NL, Lynch DA, Curran-Everett D, Brown KK, Lee KS, et al. Chronic hypersensitivity pneumonitis: differentiation from idiopathic pulmonary fibrosis and nonspecific interstitial pneumonia by using thin-section CT. Radiology. 2008;246(1):288–97.
71. Remy-Jardin M, Remy J, Gosselin B, Becette V, Edme JL. Lung parenchymal changes secondary to cigarette smoking: pathologic-CT correlations. Radiology. 1993;186(3):643–51.
72. Holt R, Schmidt R, Godwin J, Raghu G. High resolution CT in respiratory bronchiolitis-associated interstitial lung disease. J Comput Assist Tomogr. 1993; 1993:46–50.
73. Park JS, Brown KK, Tuder RM, Hale VA, King Jr TE, Lynch DA. Respiratory bronchiolitis-associated interstitial lung disease: radiologic features with clinical and pathologic correlation. J Comput Assist Tomogr. 2002;26(1):13–20.
74. Nakanishi M, Demura Y, Mizuno S, Ameshima S, Chiba Y, Miyamori I, et al. Changes in HRCT findings in patients with respiratory bronchiolitis-associated interstitial lung disease after smoking cessation. Eur Respir J. 2007;29(3):453–61.
75. Brauner MW, Grenier P, Mouelhi MM, Mompoint D, Lenoir S. Pulmonary histiocytosis X: evaluation with high-resolution CT. Radiology. 1989;172:255–8.
76. Moore AD, Godwin JD, Müller NL, Naidich DP, Hammar SP, Buschman DL, et al. Pulmonary histiocytosis X: comparison of radiographic and CT findings. Radiology. 1989;172(1):249–54.
77. Kulwiec E, Lynch D, Aguayo S, Schwarz M, King Jr TE. Imaging of pulmonary histiocytosis X. Radiographics. 1992;12:515–26.
78. Koyama M, Johkoh T, Honda O, Tsubamoto M, Kozuka T, Tomiyama N, et al. Chronic cystic lung disease: diagnostic accuracy of high-resolution CT in 92 patients. AJR Am J Roentgenol. 2003;180(3):827–35.
79. Bergin CJ, Coblentz CL, Chiles C, Bell DY, Castellino RA. Chronic lung diseases: specific diagnosis by using CT. AJR Am J Roentgenol. 1989;152(6):1183–8.
80. Lenoir S, Grenier P, Brauner MW, Frija J, Remy JM, Revel D, et al. Pulmonary lymphangiomyomatosis and tuberous sclerosis: comparison of radiographic and thin-section CT findings. Radiology. 1990;175(2):329–34.
81. Aberle DR, Hansell DM, Brown K, Tashkin DP. Lymphangiomyomatosis: CT, chest radiographic, and functional correlations. Radiology. 1990;176(2):381–7.

82. Müller NL, Chiles C, Kullnig P. Pulmonary lymphangiomyomatosis: correlation of CT with radiographic and functional findings. Radiology. 1990; 175(2):335–9.
83. Rappaport D, Weisbrod G, Herman S, Chanberlain D. Pulmonary lymphangioleiomyomatosis: high-resolution CT findings in four cases. AJR Am J Roentgenol. 1989;152:961–4.
84. Sherrier RH, Chiles C, Roggli V. Pulmonary lymphangioleiomyomatosis: CT findings. AJR Am J Roentgenol. 1989;153(5):937–40.
85. Templeton PA, McLoud TC, Müller NL, Shepard JA, Moore EH. Pulmonary lymphangioleiomyomatosis: CT and pathologic findings. J Comput Assist Tomogr. 1989;13(1):54–7.
86. Avila NA, Kelly JA, Chu SC, Dwyer AJ, Moss J. Lymphangioleiomyomatosis: abdominopelvic CT and US findings. Radiology. 2000;216(1):147–53.
87. Avila NA, Dwyer AJ, Rabel A, Moss J. Sporadic lymphangioleiomyomatosis and tuberous sclerosis complex with lymphangioleiomyomatosis: comparison of CT features. Radiology. 2007;242(1): 277–85.
88. Chang AB, Masel JP, Masters B. Post-infectious bronchiolitis obliterans: clinical, radiological and pulmonary function sequelae. Pediatr Radiol. 1998; 28(1):23–9.
89. Lynch D, Brasch R, Hardy K, Webb W. Pediatric pulmonary disease: assessment with high-resolution ultrafast CT. Radiology. 1990;176:243–8.
90. Lynch D, Hay T, Newell Jr JD, Divgi V, Fan L. Pediatric diffuse lung disease: diagnosis and classification by high-resolution CT. AJR Am J Roentgenol. 1999;173:713–8.
91. Padley SP, Adler BD, Hansell DM, Müller NL. Bronchiolitis obliterans: high resolution CT findings and correlation with pulmonary function tests. Clin Radiol. 1993;47(4):236–40.
92. Worthy SA, Park CS, Kim JS, Müller NL. Bronchiolitis obliterans after lung transplantation: high-resolution CT findings in 15 patients. AJR Am J Roentgenol. 1997;169(3):673–7.
93. Reittner P, Müller NL, Heyneman L, Johkoh T, Park JS, Lee KS, et al. Mycoplasma pneumoniae pneumonia: radiographic and high-resolution CT features in 28 patients. AJR Am J Roentgenol. 2000;174(1): 37–41.
94. Akira M, Higashihara T, Sakatani M, Hara H. Diffuse panbronchiolitis: follow-up CT examination. Radiology. 1993;189(2):559–62.

http://www.springer.com/978-1-4419-9770-8

Diffuse Lung Disease
A Practical Approach
Baughman, R.P.; du Bois, R.M. (Eds.)
2012, XII, 400 p. 166 illus., 80 illus. in color., Hardcover
ISBN: 978-1-4419-9770-8